ACS OMEGA

Open Access

http://pubs.acs.org/journal/acsodf

Article

Real-Time Monitoring of Electrode Surface Changes in Fast-Scan Cyclic Voltammetry Using Fourier Transform Electrochemical Impedance Spectroscopy

Cheonho Park,[▽] Youngjong Kwak,[▽] Jaehyun Jang, Sangmun Hwang, Hyun U Cho, Se Jin Jeon, Yoonbae Oh, Hojin Shin, Kendall H. Lee, and Dong Pyo Jang*

Cite This: *ACS Omega* 2025, 10, 2061−2068

Read Online

ACCESS | Metrics & More | Article Recommendations | Supporting Information

ABSTRACT: Fast-scan cyclic voltammetry (FSCV) is a widely used electrochemical technique to measure the phasic response of neurotransmitters in the brain. It has the advantage of reducing tissue damage to the brain due to the use of carbon fiber microelectrodes as well as having a high temporal resolution (10 Hz) sufficient to monitor neurotransmitter release in vivo. During the FSCV experiment, the surface of the carbon fiber microelectrode is inevitably changed by the fouling effect. In terms of redox peak potential and sensitivity against neurotransmitters, a changed electrode surface results in a voltammogram that differs from the precalibration. However, when an electrode is implanted in the brain, the method for monitoring the electrode status change is limited. In this study, we propose employing an electrochemical impedance concept to monitor the gradual change of the electrode surface during FSCV scanning. Fourier transform electrochemical impedance spectroscopy (FTEIS) was used in combination with FSCV to detect the real-time impedance of the electrode. The relationship between impedance and electrode surface conditions was studied by immersing carbon fiber microelectrodes in bovine serum albumin solution to induce biofouling and diminish electrode sensitivity. As a result of the nonspecific adsorption of bovine serum albumin during the interleave scan of FSCV and FTEIS, both the measured dopamine response and the capacitance of the equivalent circuit model from FTEIS decreased over time. The capacitance and sensitivity of the electrode showed correlation (R^2 = 0.90), while the resistance of the equivalent circuit did not. In vivo measurements using the interleave scan of FSCV and FTEIS were also carried out to observe biofouling on the FSCV electrode surface and to measure dopamine sensitivity in the striatum of the rat brain for an hour. The results showed that the resistance did not significantly change, while capacitance and measured dopamine were significantly diminishing over time. In summary, real-time neurotransmitter measurements and electrode monitoring with the combination of FSCV and FTEIS would be useful in neuroscience research.

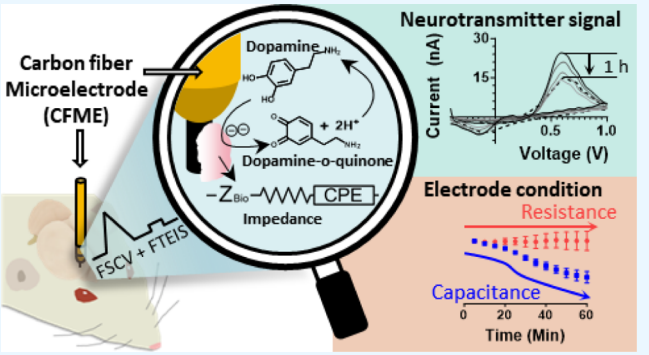

INTRODUCTION

Fast-scan cyclic voltammetry (FSCV), which is an advanced cyclic voltammetry with a fast scan rate (>400 V/s), has been frequently used to measure electroactive neurotransmitters with subsecond temporal resolution (10 Hz).[1,2] Utilizing the spatial resolution of microscale carbon fiber microelectrode (CFME) and temporal resolution, a variety of electroactive neurotransmitters like dopamine, adenosine, and serotonin have been measured using FSCV.[3−5] The changes in neurotransmitter levels that occur in real time provide useful information on the neurotransmitter-related mechanisms of the brain,[6−8] the dynamics of drug administration,[9−11] and the potential for using these levels as biomarkers of neurological disorders.[12−14]

The chemical environment of the brain consists of a variety of biochemicals, including proteins and the cerebrospinal fluid. These biochemicals have the potential to contaminate the surface of an electrode, a phenomenon known as biofouling.[1] Proteins may adsorb to the CFME surface and result in interference with the voltammogram shape.[15] It is also reported that the Ag/AgCl electrode, a commonly used reference electrode, showed dichlorination during the experiment, so the ability as a reference became poor after the insertion of Ag/AgCl into the brain.[16] Electrochemical products of neurotransmitters such as serotonin[5,17] and melatonin[18] and histamine[19] are also reported to have

Received: September 11, 2024
Revised: November 26, 2024
Accepted: December 26, 2024
Published: January 9, 2025

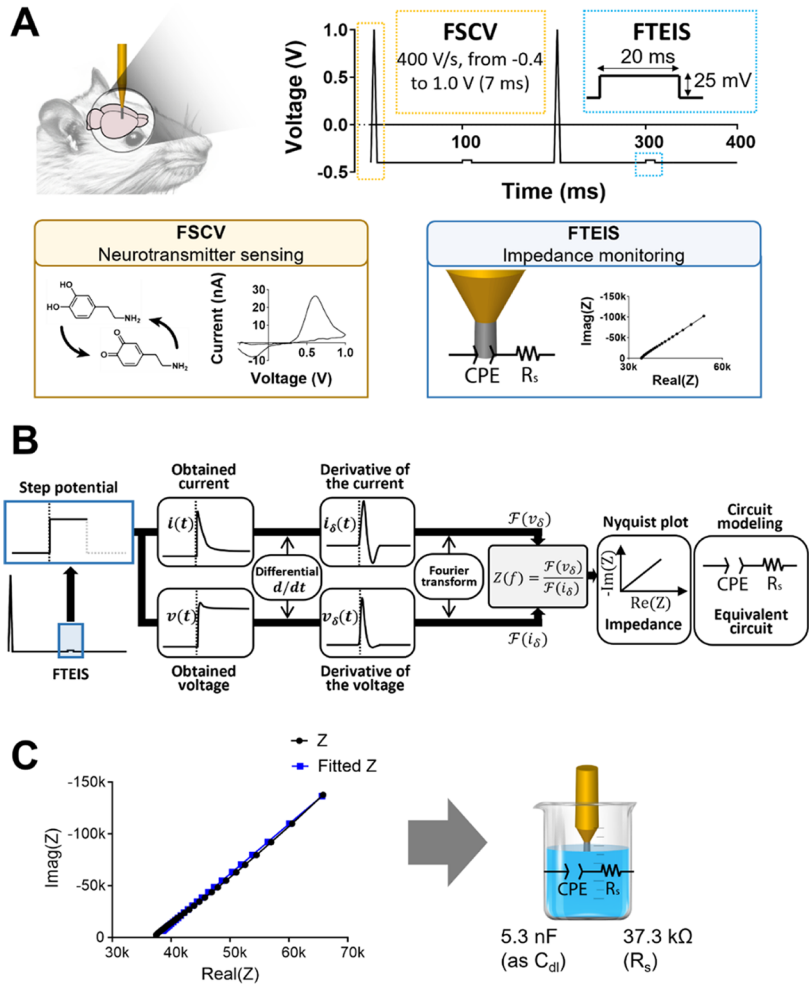

Figure 1. Graphical scheme of FSCV and FTEIS. (A) Basic concept of combining FSCV and FTEIS waveform potential. (B) FTEIS computation process to derive impedance and equivalent circuit. (C) Example of obtained impedance and fitted equivalent circuit.

adsorptive properties to the electrode, interfering with signals. During the FSCV experiment, the sensitivity of the electrode would inevitably alter due to biofouling. Inconsistency between precalibration and postcalibration for the concentration to voltammogram is a commonly reported issue.[9,20,21] When it comes to the calibration process, the postcalibration data should be taken into consideration rather than the precalibration data because the used electrode can have biofouling remnants on its surface, which would simulate the attenuated sensitivity like in vivo environment.[22]

The phenomenon implies that the sensitivity of CFME in vivo is changing during the experiment, making it difficult to accurately calibrate the measured neurotransmitter during the experiment.[20] Therefore, to obtain accurate measurements in the brain environment, it is necessary to comprehend and quantify the influence of biofouling during the FSCV experiment. There have been several studies regarding estimating the sensing ability of CFME for FSCV measurement. The summation of background current was demonstrated to be useful for calculating the active surface area of the electrode, presuming that the area is proportional to the neurotransmitter sensitivity.[23] Furthermore, background current data were used as a training set for principal component regression (PCR), allowing PCR to more precisely estimate dopamine sensitivity. It was also reported that the peak potential of background current could be used to estimate shifted dopamine peak potential during in vivo experiments.[24] These studies tried to figure out the general principle to estimate the electrode status, and they all proposed capacitive current as an indicator of electrode status.

Monitoring the functional change of the electrode could be approached from a different perspective: electrochemical impedance. Electrochemical impedance spectroscopy (EIS) is a technique that reduces the complexity of an electrochemical system to an equivalent circuit consisting of resistance, capacitance, and additional electrical components. EIS has several advantages over other electrochemical techniques, including the ability to provide information about both the kinetics and thermodynamics of electrochemical reactions.[25−27] This approach has the advantage of providing explainable information on the electrochemical system. Recent FSCV studies examined biofouling from the standpoint of electrochemical impedance, showing that the impedance had been changed because of biofouling during the experiment.[28,29] It is also notable that the biofouling effect could be simulated by using additional electric circuits in the FSCV measuring systems; thereby the dopamine voltammograms showed sensitivity loss and oxidation peak shift as the impedance changed.[16,24] FSCV studies using impedance concepts have the potential to understand how and what factors affect the FSCV measurement more than investigating the capacitive current. In our prior work, we measured impedance using Fourier

https://doi.org/10.1021/acsomega.4c08240
ACS Omega 2025, 10, 2061−2068

transform electrochemical impedance spectroscopy (FTEIS) and neurotransmitters using fast cyclic square wave voltammetry (FCSWV).[30,31] FTEIS is an electrochemical technique that was developed to improve the temporal resolution of EIS and is based on the application of a simple step-pulse waveform instead of using sinusoidal waveforms with multiple frequencies as conventional EIS scans.[32,33] The FTEIS processing includes differential and Fourier transforms of the applied step pulse voltage and its current response to obtain the impedance of the entire frequency.[34,35] Our previous study focused on deriving new features using FTEIS from square wave cyclic voltammetry to help chemometric analysis, but the square wave voltammetry had a large amplitude enough to have not only impedance information but also redox information. In this study, small-amplitude FTEIS as an impedance measuring technique was combined with FSCV to observe impedance information only. The combination would benefit from the temporal resolution of both electrochemical methods, monitoring neurotransmitter concentrations and estimating system impedance.

RESULTS AND DISCUSSION

Optimization of Interleave Scan of FSCV and FTEIS. In this study, we proposed Fourier transform electrochemical impedance spectroscopy (FTEIS) in conjunction with FSCV for faster impedance scanning during FSCV scanning (Figure 1A). FTEIS was developed to improve the temporal resolution of electrochemical impedance spectroscopy (EIS) by using a step pulse instead of multiple sinusoidal pulses from the conventional EIS.[33] The main notion of FTEIS is to obtain impedance information by applying an impulse response. An impulse is usually modeled as a delta function, which has an infinite amplitude and a very short duration. When an impulse is applied to a system, the system's response is known as the impulse response. The impulse response provides information on how the system behaves in response to a brief input signal and can be used to characterize the dynamic behavior of the system.[36] Nevertheless, it is challenging to apply an impulse to a real system because an impulse has infinite value. Park and Yoo[33] employed a step pulse to avoid the infinite value problem based on the idea that the step function is an integrated form of the delta function. The current response to the step pulse perturbation is processed using the differential and Fourier transforms to produce the pseudoimpulse response.[31] In comparison to the conventional EIS, this approach has a higher temporal resolution. Considering the subsecond time resolution of neurotransmitter release, FTEIS has the potential to be employed simultaneously with FSCV to study neurotransmitters and impedance at subsecond temporal resolution. As a result, in this study, the FSCV scan and FTEIS scan are performed alternatively (Figure 1A).

Selecting step pulse parameters for subsecond temporal resolution of FSCV was the initial step in implementing FTEIS to the FSCV experiment. Increasing the amplitude of the step pulse directly enhances the signal-to-noise ratio, resulting in more precise impedance. The amplitude, on the other hand, has the possible disadvantage of including Faradaic reactions at the redox potential by widening the scanning range and violating linearity, which is one of the key conditions of EIS. Therefore, we chose 25 mV as the perturbation amplitude, such that the impedance can only be used to collect system information. The duration of the step pulse was another parameter that had to be selected. Increasing the duration will result in better frequency resolution in the impedance information on FTEIS, but it may contaminate the next FSCV scan with the remaining decaying current of the longer step pulse. Therefore, we chose a short duration of 20 ms as the step pulse duration. Theoretically, FTEIS provides the total impedance; however, because the duration of the employed step pulse is very short (20 ms) for subsecond monitoring of impedance, obtaining whole impedance for all frequencies was not achievable as a trade-off. Therefore, the range of frequencies gathered for FTEIS had to be limited to a certain range of frequencies rather than analyzing all frequencies. First, in the case of a minimum low frequency, the duration of the step pulse posed a limitation. It is implausible that a step pulse with a period of 20 ms would produce impedance with a frequency of 50 Hz or less. As a result, in the case of low frequency, impedances with frequencies below 150 Hz were discarded to ensure that unreliable impedances were not considered. In addition, the electrochemical measurement system employs voltammetric hardware with a defined effective frequency response boundary (known as the cutoff frequency), which serves as a critical parameter for assessing the impedance. When AC sweeping was utilized with the potentiostat, the voltage−current ratio exhibited distortion beyond 20 kHz (refer to Figure S1). Due to this restricted frequency response, details regarding high-frequency impedance should also be disregarded. Consequently, the impedance acquired through FTEIS measurements in this study was constrained within the range of 150−20 kHz.

Measuring changes in impedance, which involves shifts in both real and imaginary components across different frequencies on a complex plane, can be challenging to quantify accurately. To address this, we employed equivalent circuit modeling based on the FTEIS data. In our FSCV system, we opted for a specific circuit—a series of a resistor (R) and a constant phase element (CPE)—to fit the impedance instead of the general Randles circuit (Figure 1B), as suggested in previous FSCV/impedance studies[28,29] (see Supporting eq 1). The CPE is a theoretical tool used to explain how the electrode behaves like a pseudocapacitor. Integrating the CPE into the electrode's electrical circuit allows us to accurately measure the impedance of CFME. To simplify the understanding of the CPE, we converted it to a double-layer capacitance (C_{dl}) using specific characteristics of the CPE, such as the characteristic parameter (Q0), shifted phase (n), and resistance (R) (Supporting Information).[37] During our experiments that monitored biofouling, we observed changes in both resistance and capacitance within the R-CPE circuit. This helped us determine which parameter significantly affects the sensitivity of the electrode.

FTEIS Feasibility in Monitoring the Electrode Surface Change. The next step in adapting FTEIS to FSCV was to check whether FTEIS could effectively monitor changes on the electrode surface. Biofouling in the brain would be the most common form of electrode surface change during the FSCV experiment. To simulate this, we used a solution containing 40 g per liter of bovine serum albumin (BSA) for two reasons. First, protein is regarded as an important factor in biofouling to be studied since nonspecific protein adsorption is critical in the early step of the electrode encapsulation process in the brain to induce further biofouling.[38] Second, BSA has been used as a biofouling source in previous FSCV and biosensor research.[39,40] For the FSCV experiment, the dopamine FSCV waveform (from −0.4 to 1.0 V, 400 V/s) was used instead of

https://doi.org/10.1021/acsomega.4c08240
ACS Omega 2025, 10, 2061−2068

the conventional dopamine waveform (from −0.4 to 1.3 V, 400 V/s) to accelerate biofouling because the peak potential of 1.3 V of the conventional waveform has been adopted for resurfacing ability to prevent and remove biofouling.[41]

Before BSA biofouling processing, a voltammogram of 1 μM dopamine (DA) in Tris buffer solution was measured to obtain reference data. Then, the electrodes were immersed in BSA-Tris solution for 30 min while applying FSCV to induce biofouling on the electrode. After the biofouling process, the electrode was transferred to the buffer solution, and the impedance and the dopamine response to 1 μM DA solution were measured. Following that, the biofouling and monitoring protocols were repeated four times. During this process, it was confirmed that dopamine sensitivity decreased by an average of 56% from the initial measurement (Figure 2A). From the

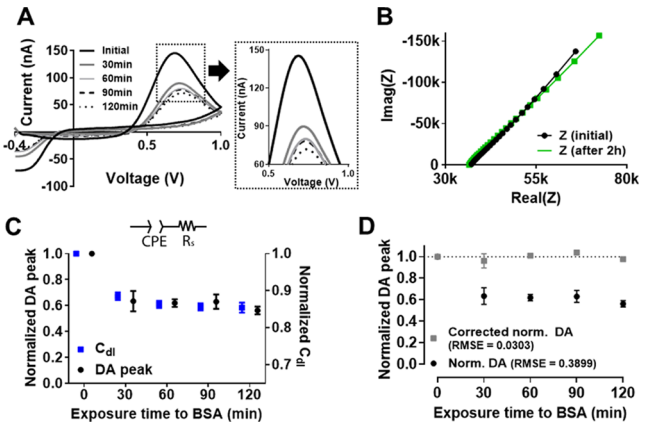

Figure 2. BSA biofouling estimation was carried out with FTEIS. (A) Voltammogram over time for the same amount of dopamine solution (1 μM). (B) Impedance measurements before and after the experiment. (C) The peak dopamine (DA) voltammogram over time and the standardized capacitance over time. (D) Corrected dopamine signal change based on capacitance. Root mean square errors (RMSE) were calculated by subtracting between the corrected/uncorrected dopamine signals from 1.0, which represents the actual dopamine level.

impedance point of view, the Nyquist plot changed during the experiment. After 2 h of the biofouling process, the impedance increased compared to the impedance before BSA biofouling (Figure 2B). The capacitance and resistance from the fitted R-CPE circuit were shown to quantify the change in impedance (Figure 2C). The capacitance decreased with the biofouling, and it showed a significant relationship compared to DA sensitivity loss. Capacitance and impedance are inversely proportional; therefore, Figure 2B could be interpreted as an indication of decreasing capacitance. The correlation between the decrease in sensitivity and the change in capacitance caused by this nonspecific protein adsorption yields a similar result as our previous study about the application of FTEIS to square wave voltammetry.[31] Compared to capacitance, the resistance R did not change during the experiment (Figure 3).

This relationship between capacitance and dopamine sensitivity is also consistent with previous FSCV studies using total capacitive current.[23,42] These studies showed that there is a positive correlation between the total capacitive current and the sensitivity of the electrode against dopamine. In general, the capacitance of the electrode is used to estimate the performance of the electrode because the capacitance is related to the electrochemically active surface area available for charge transfer.[43] Physically, the biofouling component sticks to the electrode first, and then, there are two things that happen: first, the insulating effect of the biofouling component will change the conductivity, which will change the measured capacitance, and second, the biofouling component will block the active site of the electrode, which will have the effect that we know as the biofouling effect, which is that the electrode will measure less analyte. From our results, the capacitance decreased during the biofouling experiment, which means that the active area of the electrode is blocked by protein and therefore the capacitance decreased. After the biofouling experiment in the Tris buffer, C_{dl} and dopamine peak data were utilized in a simple linear regression analysis. Using the decrease in C_{dl} as a variable, the resulting equation made it possible to estimate the sensitivity according to the change in the amount of C_{dl} (R^2 = 0.90).

Last, we demonstrate how the measured capacitance can be utilized. The normalized DA peak and the trend of normalized capacitance obtained from Figure 2D were analyzed through linear regression, and dopamine trends were adjusted using the ratio of the slopes of the two linear functions. In Figure 2D, as a result of this correction process, the decreasing dopamine trend was adjusted to reflect a more average value (the distribution of corrected dopamine signal (mean ± standard deviation): 0.996 ± 0.035). To evaluate the corrected normalized dopamine signals, the root-mean-square error (RMSE) was calculated by subtracting corrected values from 1, which represented the actual dopamine level.

Monitoring Biofouling In Vivo. Then, the interleave scan of FSCV and FTEIS in in vivo experiment was conducted to observe the impedance change during the real biofouling environment as a proof of concept (n = 3). The evoked dopamine response caused by electrical stimulation of the medial forebrain bundle (MFB, from bregma, AP: −4.6 mm, ML: 1.4 mm, from dura, DV: −8.0 to approximately −9.0 mm) in rats was measured in the striatum (AP: 1.2 mm, ML: 2.0 mm, DV: −4.5 mm) to monitor the DA sensitivity. Electrical stimulation was delivered at 5-min intervals and recorded for 1 h (Figure 3A,B). The dopamine signal was identified through the peak signal at 0.5−0.6 V, which is the oxidation characteristic of dopamine. The dopamine peak exhibited a gradual decrease over the duration of the experiment, as anticipated. Although it is challenging to assume that every evoked dopamine response has identical concentration levels, it is often anticipated that there will be a similar response after a sufficient period of resting time between each stimulation (>5 min), but the dopamine response was diminishing (Figure 3C). Similar to the BSA solution experiment, impedance increased during 1 h of recording (Figure 3D). As described above, an increase in the impedance can be caused by a drop in the capacitance, which indicates a reduction in the active surface area of the electrode. The impedance scale in this experiment differs from the prior experiment in the buffer solution. This is because the electrode used in the studies had smaller dimensions, as described in the Methods section.

The dopamine peak was normalized and averaged to show a change during the experiment. As a result of the experiment, both the evoked dopamine response and C_{dl} steadily reduced over time (Figure 3F,G). Despite the expectation of a consistent dopamine response, the initial concentration was not maintained due to biofouling. As a result, the biofouling resulted in errors in the estimated concentration for the

https://doi.org/10.1021/acsomega.4c08240
ACS Omega 2025, 10, 2061−2068

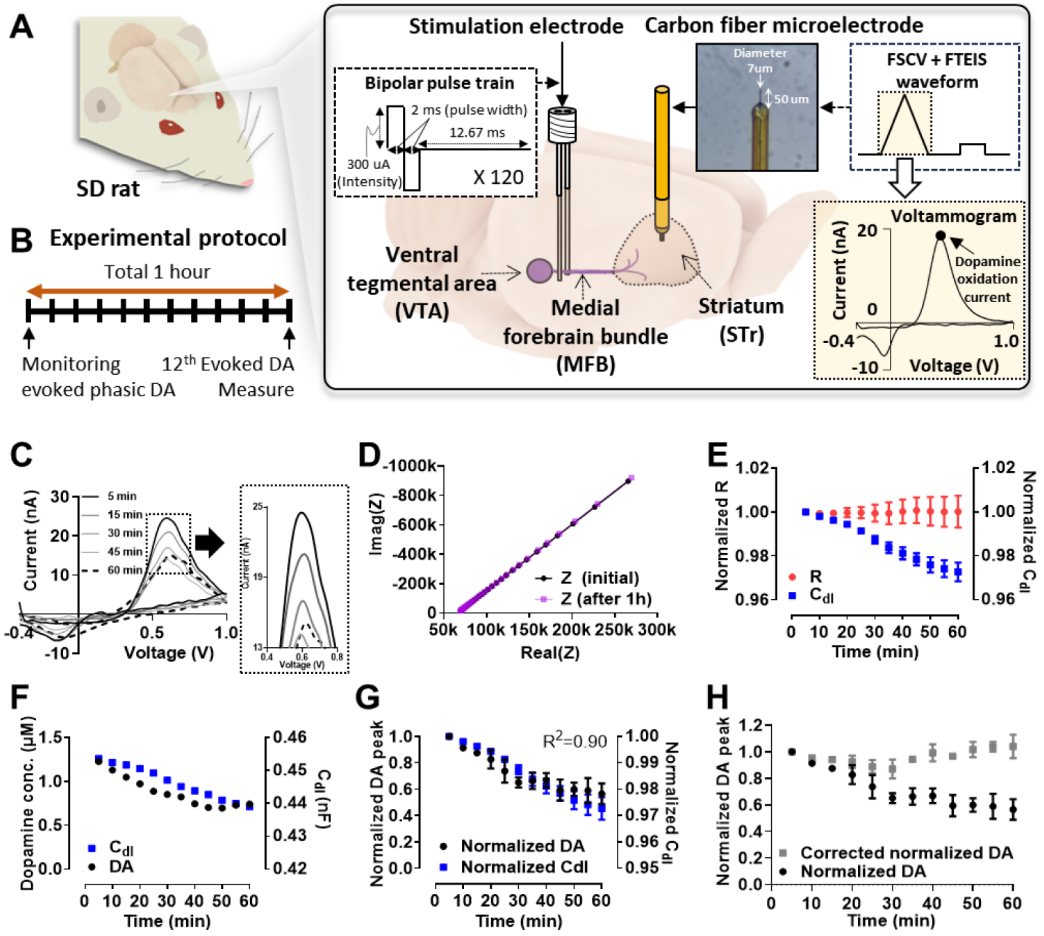

Figure 3. Graphical explanation of the in vivo biofouling experiment. (A) An illustration of the electrically stimulated areas in the brains of rats, together with the stimulation settings and the subsequent dopamine voltammograms. (B) Experimental protocol. Evoked dopamine levels were assessed at 5-min intervals throughout a 1-h experiment. (C) Example of DA voltammograms over time during the experiment. (D) Impedance at the onset of the experiment and after 1 h. (E) Estimation of changes in resistance and capacitance over time using FTEIS. (F) Temporal changes in dopamine release and capacitance measurements obtained from a single rat. (G) Temporal changes in dopamine release and capacitance. Both dopamine and capacitance were normalized (n = 3). (H) Corrected dopamine signal change based on capacitance.

dopamine response. Resistance and capacitance change were also simultaneously shown in Figure 3E, but resistance did not change as we observed the phenomenon in the BSA biofouling experiment. An additional experiment was conducted as a control, employing a relatively high peak voltage waveform known for its resurfacing capability (−0.4 to 1.3 V, 400 V/s). We also observed a change in capacitance with the diminution of the dopamine response in this experiment from the result; however, the change was more gradual and less noticeable than that observed with the 1.0 V peak waveform (Figure S2). The experimental findings of the control group indicate that the capacitance and electrode surface area remain relatively unchanged because of the resurfacing capability exhibited by the 1.3 V peak waveform.

When comparing the results of in vivo and ex vivo experiments, we observe that capacitance reduction is approximately 3% in the in vivo experiment, while it is approximately 15% in the ex vivo experiment. However, directly comparing these two biofouling models and expecting them to show the same capacitance changes have limitations. In this study, bovine serum albumin (BSA) performed well as a biofouling agent, but this does not imply that BSA fully replicates the biofouling process observed in vivo. In an in vivo environment, the protein concentration differs, and other biochemicals, in addition to proteins, also contribute to biofouling. In this context, the contribution of each chemical to the capacitance change and electrode sensitivity will vary. Capacitance change reflects the conductivity of the substance adhering to the electrode, while dopamine sensitivity relates to how much the adhering substance blocks the active site. Therefore, the degree of biofouling in ex vivo and in vivo experiments will differ by biofouling components. Another factor that may have influenced these results is the timing of the biofouling experiments. The ex vivo experiment was conducted under fully controlled conditions, allowing us to observe the electrode sensitivity before biofouling occurred, whereas the in vivo experiment took place after a stabilization process in the brain, resulting in a different degree of initial fouling status compared to the ex vivo setup.

The correlation between changes in capacitance and decreased dopamine sensitivity does not imply causality. The alterations in dopamine sensitivity caused by biofouling are influenced by several factors, including biological changes and variations in the electrode conditions. In our study, we aimed to simultaneously gather both dopamine sensitivity and impedance data, working on a technique to partially correct the decreased dopamine sensitivity based on impedance changes.

https://doi.org/10.1021/acsomega.4c08240
ACS Omega 2025, 10, 2061−2068

Finally, we demonstrate the potential application of the measured capacitance in in vivo experiments, similar to the approach used in in vitro experiments. The normalized DA peak and normalized capacitance trends presented in Figure 3G were analyzed using linear regression, and the dopamine trends were corrected based on the ratio of the slopes of the two linear functions. In Figure 3H, the decreasing dopamine trends resulting from this correction were adjusted to yield a more representative average value. This simple correction process can help mitigate the effects of biofouling during long-term experiments (e.g., >1 h), thereby partially restoring the sensitivity of the measurements.

CONCLUSION

Combining the rapid impedance measuring technique with FSCV was proposed as a strategy for real-time monitoring of the functional change of the electrode surface while measuring the change of the neurotransmitter. FTEIS was adjusted to the subsecond temporal resolution of FSCV in the limited frequency range with short pulse duration for real-time measurement. The frequency response from FTEIS is then used to fit the equivalent circuit to find pseudocapacitance (CPE) and resistance. To illustrate its applicability, the carbon fiber microelectrode was subjected to the biofouling impact of BSA, and the consequences of biofouling were observed for both FSCV and FTEIS. Consequently, dopamine sensitivity decrease was shown to have a positive correlation against capacitance derived from R-CPE circuit fitting, while the resistance did not. The in vivo experiment showed consistent results compared to the experiment using BSA. Both dopamine sensitivity and capacitance decreased for 1 h in the rat brain. In summary, the utilization of FTEIS for the capacitance calculation during FSCV scanning enables the precise quantification of electrode degradation throughout the experiment.

EXPERIMENTAL SECTIONS

Data Acquisition. Data were acquired using a commercial electronic interface (NI USB-6356, 16-bit, National Instruments) connected to a base-station PC, alongside custom software developed in the LabVIEW programming environment (National Instruments, Austin, TX). To minimize impedance information loss in the step pulse of FTEIS, a current-to-voltage converting preamplifier without any analogue filter was employed. Following data collection, custom software was used to control all waveform parameters and operations, data acquisition and transmission, background subtraction, and signal averaging. The collected data were saved to the hard drive of the base-station computer for offline processing in MATLAB (MathWorks Inc., Natick, MA). GraphPad Prism (GraphPad Software, San Diego, CA) was utilized to generate the figures and perform statistical analyses.

Electrodes. A carbon fiber (d = 30 μM, World Precision Instruments, FL, US) was used in the ex vivo experiment for a better signal-to-noise ratio. The detailed fabrication process has been described in our previous paper.[31] The exposed carbon fiber was trimmed to a final length of 100 μm using a scalpel. After 4 h of conditioning, CFME was employed in the ex vivo experiment. For the in vivo study, the carbon fiber with a smaller diameter (d = 7 μM, Hexel, Stamford, CT) was used to minimize cell damage. The exposed carbon fiber was trimmed to a final length of 50 μM with a scalpel. For the CFME in the in vivo experiment, an additional conditioning process in the brain was added for 1 h to minimize the background drift. The Ag/AgCl reference electrode was fabricated by chlorinating 1 mm of the bare end of a 31-gauge silver wire (PFA coated 030″, bare 025″, A-M Systems).

Interleave Scan of FSCV and FTEIS. Conventional dopamine waveform (400 V/s, from −0.4 to 1.3 V) has the resurfacing ability to prevent sensitivity change.[41] To enhance the change of sensitivity during the short-time window of the experiment (1−2 h), an old dopamine waveform (400 V/s, from −0.4 to 1.0 V) was adopted. We employed the FSCV waveform with a switching potential at 1.0 V because FTEIS was performed to see the condition of the electrode surface. However, FSCV with a 1.3 V switching potential could make the surface of the electrode resurface through high voltage. A step pulse for FTEIS was inserted between each FSCV scan during the holding potential, as shown in Figure 1A. The repetition frequency was reduced to 5 Hz instead of 10 Hz, which is the conventional parameter. The step pulse of 20 ms (−0.4 V to −0.375 V) was added between each FSCV triangular scan. The background subtraction method was used to obtain the dopamine response during the experiments.[44]

FTEIS Equivalent Circuit Estimation. All impedance data in the study were fitted using Zfit, which is a MATLAB algorithm developed to fit the electrochemical impedance.[45] The equivalent circuit was composed of a serial circuit of resistance R and constant phase element CPE to fit the unique shape of the Nyquist plot obtained in the experiment. The detailed explanation of choosing the circuit is given in the Results and Discussion section.

Dopamine Signal Correction. To correct for the decreasing dopamine sensitivity, normalized dopamine peak values and normalized C_{dl} values obtained from in vivo experiments were used. The changes in the optimized dopamine peak and C_{dl} values were fitted using simple linear regression (eqs 1 and2).

$$DA_{peak}(t) = Grad_{DA} \times t + 1 \tag{1}$$

$$C_{dl}(t) = Grad_{C} \times t + 1 \tag{2}$$

where DA_{peak} and C_{dl} represent the normalized dopamine peak current and capacitance values at a specific time, while $Grad_{DA}$ and $Grad_{C}$ represent the optimized rate of change for DA_{peak} and C_{dl}, respectively, measured during the protocol. Based on these two equations, the following correlation (eq 3) can be established. Assuming no change in dopamine sensitivity due to biofouling, a corrected dopamine value can be obtained, as shown in eq 4.

$$DA_{peak} = (C_{dl} - 1) \times \frac{Grad_{DA}}{Grad_{C}} + 1 \tag{3}$$

$$DA_{corrected} = DA_{peak} - (C_{dl} - 1) \times \frac{Grad_{DA}}{Grad_{C}} \tag{4}$$

Chemicals. Dopamine was dissolved at a stock concentration of 1 mM in Tris buffer (15 mM Tris (hydroxymethyl) aminomethane, 3.25 mM KCl, 140 mM NaCl, 1.2 mM $CaCl_2$, 1.25 mM NaH_2PO_4, 1.2 mM $MgCl_2$, and 2.0 mM Na_2SO_4, pH 7.4). The stock dopamine solution was diluted to the final concentration in the Tris buffer during the experiment. Bovine serum albumin (BSA) solution was produced by adding BSA

https://doi.org/10.1021/acsomega.4c08240
ACS Omega 2025, 10, 2061−2068

to Tris buffer at a concentration of 40 g/L.[39] All chemicals were purchased from Sigma-Aldrich (St. Louis, MO).

In Vivo Experiments. Adult male Sprague−Dawley rats (8−9 weeks old, weighing 300−400 g, Orientbio, South Korea) were used for this study. The rats were housed in 12-h light/dark cycles and were given food and water ad libitum. US National Institutes of Health (NIH) guidelines were followed for animal care, and the Hanyang University Institutional Animal Care and Use Committee approved the experimental procedures. Rats were anesthetized by intraperitoneal injection (anesthetic urethane, 1.5 g/kg, i.p.). Surgeries were performed using a stereotaxic frame (Model 900, David Kopf Instruments, Tujunga, CA). To evoke DA release, the medial forebrain bundle (from bregma, AP: −4.6 mm, ML: 1.4 mm, from dura, DV: −8.0 to approximately −9.0 mm) was electrically stimulated, and a CFME was inserted into the striatum (AP: 1.2 mm, ML: 2.0 mm, DV: −4.5 mm). Stimulation consisted of 120 biphasic pulses with a repetition frequency of 60 Hz; each pulse had a 2 ms duration, and the amplitude was 0.3 mA.

■ ASSOCIATED CONTENT

Supporting Information

The Supporting Information is available free of charge at https://pubs.acs.org/doi/10.1021/acsomega.4c08240.

The result of the AC sweeping experiment on the electrochemical system used in the study (Figure S1); capacitance changes over time using different FSCV waveforms (n = 3, for each individual waveform) (Figure S2); resistance and capacitance changes over time during the BSA fouling test (Figure S3); C_{dl} converting equation (Eq S1); abbreviation summary (Table S1) (PDF)

■ AUTHOR INFORMATION

Corresponding Author

Dong Pyo Jang − *Department of Biomedical Engineering, Hanyang University, Seoul 04763, Republic of Korea; Department of Electronic Engineering, Hanyang University, Seoul 04763, Republic of Korea;* orcid.org/0000-0002-2832-2576; Email: dongpjang@hanyang.ac.kr

Authors

Cheonho Park − *Department of Chemistry, University of Virginia, Charlottesville, Virginia 22901, United States*

Youngjong Kwak − *Department of Biomedical Engineering, Hanyang University, Seoul 04763, Republic of Korea; Department of Biomedical Engineering, Mayo Clinic, Rochester, Minnesota 55902, United States;* orcid.org/0009-0005-6016-4490

Jaehyun Jang − *Department of Electronic Engineering, Hanyang University, Seoul 04763, Republic of Korea*

Sangmun Hwang − *Department of Biomedical Engineering, Hanyang University, Seoul 04763, Republic of Korea*

Hyun U Cho − *Department of Biomedical Engineering, Hanyang University, Seoul 04763, Republic of Korea*

Se Jin Jeon − *Department of Pharmacology, College of Medicine, Hallym University, Chuncheon 24252, Republic of Korea*

Yoonbae Oh − *Department of Biomedical Engineering, Mayo Clinic, Rochester, Minnesota 55902, United States; Department of Neurologic Surgery, Mayo Clinic, Rochester, Minnesota 55902, United States; Department of Brain and Cognitive Engineering, Korea University, Seoul 02841, Republic of Korea;* orcid.org/0000-0003-1779-978X

Hojin Shin − *Department of Biomedical Engineering, Mayo Clinic, Rochester, Minnesota 55902, United States; Department of Neurologic Surgery, Mayo Clinic, Rochester, Minnesota 55902, United States;* orcid.org/0000-0001-6095-5122

Kendall H. Lee − *Department of Biomedical Engineering, Mayo Clinic, Rochester, Minnesota 55902, United States; Department of Neurologic Surgery, Mayo Clinic, Rochester, Minnesota 55902, United States*

Complete contact information is available at: https://pubs.acs.org/10.1021/acsomega.4c08240

Author Contributions

[▽]C.P. and Y.K. contributed equally. This manuscript was written through the contributions of all authors. All authors have given approval to the final version of the manuscript.

Notes

The authors declare no competing financial interest.

■ ACKNOWLEDGMENTS

This research was supported by the National Institutes of Health, USA (NIH R01NS112176, R01NS129549, and R42NS125895), the National Research Foundation of Korea (NRF) grant funded by the Korean government (MSIT) (RS-2024-00339708, RS-2023-00266075), and a grant from the Korea Health Technology R&D Project through the Korea Health Industry Development Institute (KHIDI), funded by the Ministry of Health & Welfare, Republic of Korea (HI19C075300). Additionally, this research was supported by a grant from the Mental Health Related Social Problem Solving Project, funded by the Ministry of Health & Welfare, Republic of Korea (RS-2024-00413115).

■ REFERENCES

(1) Puthongkham, P.; Venton, B. J. Recent advances in fast-scan cyclic voltammetry. *Analyst* **2020**, *145* (4), 1087−1102.

(2) Venton, B. J.; Cao, Q. Fundamentals of fast-scan cyclic voltammetry for dopamine detection. *Analyst* **2020**, *145* (4), 1158−1168.

(3) Kishida, K. T.; Sandberg, S. G.; Lohrenz, T.; Comair, Y. G.; Saez, I.; Phillips, P. E. M.; Montague, P. R.; Zars, T. Sub-second dopamine detection in human striatum. *PLoS One* **2011**, *6* (8), No. e23291.

(4) Swamy, B. E.; Venton, B. J. Subsecond detection of physiological adenosine concentrations using fast-scan cyclic voltammetry. *Anal. Chem.* **2007**, *79* (2), 744−750.

(5) Dunham, K. E.; Venton, B. J. Improving serotonin fast-scan cyclic voltammetry detection: new waveforms to reduce electrode fouling. *Analyst* **2020**, *145* (22), 7437−7446.

(6) Wakabayashi, K. T.; Bruno, M. J.; Bass, C. E.; Park, J. Application of fast-scan cyclic voltammetry for the in vivo characterization of optically evoked dopamine in the olfactory tubercle of the rat brain. *Analyst* **2016**, *141* (12), 3746−3755.

(7) Park, J.; Wheeler, R. A.; Fontillas, K.; Keithley, R. B.; Carelli, R. M.; Wightman, R. M. Catecholamines in the bed nucleus of the stria terminalis reciprocally respond to reward and aversion. *Biol. Psychiatry* **2012**, *71* (4), 327−334.

(8) Wightman, R. M.; Robinson, D. L. Transient changes in mesolimbic dopamine and their association with'reward'. *J. Neurochem.* **2002**, *82* (4), 721−735.

(9) Davidson, C.; Ellinwood, E. H.; Douglas, S. B.; Lee, T. H. Effect of cocaine, nomifensine, GBR 12909 and WIN 35428 on carbon fiber microelectrode sensitivity for voltammetric recording of dopamine. *J. Neurosci. Methods* **2000**, *101* (1), 75−83.

(10) Yuen, J.; Goyal, A.; Rusheen, A. E.; Kouzani, A. Z.; Berk, M.; Kim, J. H.; Tye, S. J.; Blaha, C. D.; Bennet, K. E.; Lee, K. H.; et al. Cocaine increases stimulation-evoked serotonin efflux in the nucleus accumbens. *J. Neurophysiol.* **2022**, *127* (3), 714−724.
(11) Cho, H. U.; Kim, S.; Sim, J.; Yang, S.; An, H.; Nam, M. H.; Jang, D. P.; Lee, C. J. Redefining differential roles of MAO-A in dopamine degradation and MAO-B in tonic GABA synthesis. *Exp. Mol. Med.* **2021**, *53* (7), 1148−1158.
(12) Lee, K. H.; Lujan, J. L.; Trevathan, J. K.; Ross, E. K.; Bartoletta, J. J.; Park, H. O.; Paek, S. B.; Nicolai, E. N.; Lee, J. H.; Min, H. K.; et al. WINCS Harmoni: Closed-loop dynamic neurochemical control of therapeutic interventions. *Sci. Rep.* **2017**, *7*, 46675.
(13) Nicolai, E. N.; Trevathan, J. K.; Ross, E. K.; Lujan, J. L.; Blaha, C. D.; Bennet, K. E.; Lee, K. H.; Ludwig, K. A. Detection of Norepinephrine in Whole Blood via Fast Scan Cyclic Voltammetry. *IEEE Int. Symp. Med. Meas Appl.* **2017**, *2017*, 111−116.
(14) Bergstrom, B. P.; Sanberg, S. G.; Andersson, M.; Mithyantha, J.; Carroll, F. I.; Garris, P. A. Functional reorganization of the presynaptic dopaminergic terminal in parkinsonism. *Neuroscience* **2011**, *193*, 310−322.
(15) Roberts, J. G.; Sombers, L. A. Fast-Scan Cyclic Voltammetry: Chemical Sensing in the Brain and Beyond. *Anal. Chem.* **2018**, *90* (1), 490−504.
(16) Seaton, B. T.; Hill, D. F.; Cowen, S. L.; Heien, M. L. Mitigating the Effects of Electrode Biofouling-Induced Impedance for Improved Long-Term Electrochemical Measurements In Vivo. *Anal. Chem.* **2020**, *92* (9), 6334−6340.
(17) Shin, H.; Goyal, A.; Barnett, J. H.; Rusheen, A. E.; Yuen, J.; Jha, R.; Hwang, S. M.; Kang, Y.; Park, C.; Cho, H. U.; et al. Tonic Serotonin Measurements In Vivo Using N-Shaped Multiple Cyclic Square Wave Voltammetry. *Anal. Chem.* **2021**, *93* (51), 16987−16994.
(18) Hensley, A. L.; Colley, A. R.; Ross, A. E. Real-Time Detection of Melatonin Using Fast-Scan Cyclic Voltammetry. *Anal. Chem.* **2018**, *90* (14), 8642−8650.
(19) Puthongkham, P.; Lee, S. T.; Venton, B. J. Mechanism of Histamine Oxidation and Electropolymerization at Carbon Electrodes. *Anal. Chem.* **2019**, *91* (13), 8366−8373.
(20) Logman, M. J.; Budygin, E. A.; Gainetdinov, R. R.; Wightman, R. M. Quantitation of in vivo measurements with carbon fiber microelectrodes. *J. Neurosci. Methods* **2000**, *95* (2), 95−102.
(21) Heien, M. L. Response to Comment on "Improved Calibration of Voltammetric Sensors for Studying Pharmacological Effects on Dopamine Transporter Kinetics in Vivo". *ACS Chem. Neurosci.* **2015**, *6* (9), 1652−1656.
(22) Phillips, P. E.; Robinson, D. L.; Stuber, G. D.; Carelli, R. M.; Wightman, R. M. Real-time measurements of phasic changes in extracellular dopamine concentration in freely moving rats by fast-scan cyclic voltammetry. *Methods Mol. Med.* **2002**, *79*, 443−464.
(23) Roberts, J. G.; Toups, J. V.; Eyualem, E.; McCarty, G. S.; Sombers, L. A. In situ electrode calibration strategy for voltammetric measurements in vivo. *Anal. Chem.* **2013**, *85* (23), 11568−11575.
(24) Meunier, C. J.; Roberts, J. G.; McCarty, G. S.; Sombers, L. A. Background Signal as an in Situ Predictor of Dopamine Oxidation Potential: Improving Interpretation of Fast-Scan Cyclic Voltammetry Data. *ACS Chem. Neurosci.* **2017**, *8* (2), 411−419.
(25) Chang, B. Y.; Park, S. M. Electrochemical impedance spectroscopy. *Annu. Rev. Anal Chem.* **2010**, *3*, 207−229.
(26) Lasia, A. *Electrochemical Impedance Spectroscopy and its Applications*; Springer New York: Imprint, 2014.
(27) Park, S.-M.; Yoo, J.-S. Electrochemical impedance spectroscopy for better electrochemical measurements. *Anal. Chem.* **2003**, *75* (21), 455 A−461A.
(28) Meunier, C. J.; Denison, J. D.; McCarty, G. S.; Sombers, L. A. Interpreting Dynamic Interfacial Changes at Carbon Fiber Microelectrodes Using Electrochemical Impedance Spectroscopy. *Langmuir* **2020**, *36* (15), 4214−4223.
(29) Castagnola, E.; Robbins, E. M.; Woeppel, K. M.; McGuier, M.; Golabchi, A.; Taylor, I. M.; Michael, A. C.; Cui, X. T. Real-Time Fast Scan Cyclic Voltammetry Detection and Quantification of Exogenously Administered Melatonin in Mice Brain. *Front. Bioeng. Biotechnol.* **2020**, *8*, 602216.
(30) Park, C.; Oh, Y.; Shin, H.; Kim, J.; Kang, Y.; Sim, J.; Cho, H. U.; Lee, H. K.; Jung, S. J.; Blaha, C. D.; et al. Fast Cyclic Square-Wave Voltammetry To Enhance Neurotransmitter Selectivity and Sensitivity. *Anal. Chem.* **2018**, *90* (22), 13348−13355.
(31) Park, C.; Hwang, S.; Kang, Y.; Sim, J.; Cho, H. U.; Oh, Y.; Shin, H.; Kim, D. H.; Blaha, C. D.; Bennet, K. E.; et al. Feasibility of Applying Fourier Transform Electrochemical Impedance Spectroscopy in Fast Cyclic Square Wave Voltammetry for the In Vivo Measurement of Neurotransmitters. *Anal. Chem.* **2021**, *93* (48), 15861−15869.
(32) Han, S. H.; Rho, J.; Lee, S.; Kim, M.; Kim, S. I.; Park, S.; Jang, W.; Lee, C. H.; Chang, B. Y.; Chung, T. D. In Situ Real-Time Monitoring of ITO Film under a Chemical Etching Process Using Fourier Transform Electrochemical Impedance Spectroscopy. *Anal. Chem.* **2020**, *92* (15), 10504−10511.
(33) Yoo, J. S.; Park, S. M. An electrochemical impedance measurement technique employing Fourier transform. *Anal. Chem.* **2000**, *72* (9), 2035−2041.
(34) Johnson, J. A.; Hobbs, C. N.; Wightman, R. M. Removal of Differential Capacitive Interferences in Fast-Scan Cyclic Voltammetry. *Anal. Chem.* **2017**, *89* (11), 6166−6174.
(35) Ha, L. D.; Kim, K. J.; Kwon, S. J.; Chang, B. Y.; Hwang, S. Time-Resolved Electrochemical Impedance Spectroscopy of Stochastic Nanoparticle Collision: Short Time Fourier Transform versus Continuous Wavelet Transform. *Small* **2023**, *19* (33), No. e2302158.
(36) Rabiner, L. R.; Gold, B. *Theory and application of digital signal processing*; Prentice-Hall, Inc., 1975.
(37) Brug, G. J.; van den Eeden, A. L. G.; Sluyters-Rehbach, M.; Sluyters, J. H. The analysis of electrode impedances complicated by the presence of a constant phase element. *J. Electroanal. Chem. Interfacial Electrochem.* **1984**, *176* (1), 275−295.
(38) Grainger, D. W. All charged up about implanted biomaterials. *Nat. Biotechnol.* **2013**, *31* (6), 507−509.
(39) Vreeland, R. F.; Atcherley, C. W.; Russell, W. S.; Xie, J. Y.; Lu, D.; Laude, N. D.; Porreca, F.; Heien, M. L. Biocompatible PEDOT: Nafion Composite Electrode Coatings for Selective Detection of Neurotransmitters in Vivo. *Anal. Chem.* **2015**, *87* (5), 2600−2607.
(40) Wisniewski, N.; Reichert, M. Methods for reducing biosensor membrane biofouling. *Colloids Surf., B* **2000**, *18* (3), 197−219.
(41) Heien, M. L.; Phillips, P. E.; Stuber, G. D.; Seipel, A. T.; Wightman, R. M. Overoxidation of carbon-fiber microelectrodes enhances dopamine adsorption and increases sensitivity. *Analyst* **2003**, *128* (12), 1413−1419.
(42) Schuweiler, D. R.; Howard, C. D.; Ramsson, E. S.; Garris, P. A. Improving in Situ Electrode Calibration with Principal Component Regression for Fast-Scan Cyclic Voltammetry. *Anal. Chem.* **2018**, *90* (22), 13434−13442.
(43) Bard, A. J.; Faulkner, L. R.; White, H. S. *Electrochemical Methods: fundamentals and Applications*; Wiley, 2022.
(44) Robinson, D. L.; Venton, B. J.; Heien, M. L.; Wightman, R. M. Detecting subsecond dopamine release with fast-scan cyclic voltammetry in vivo. *Clin. Chem.* **2003**, *49* (10), 1763−1773.
(45) Dellis, J.-L. *Zfit*https://www.mathworks.com/matlabcentral/fileexchange/19460-zfit).

https://doi.org/10.1021/acsomega.4c08240
ACS Omega 2025, 10, 2061−2068